Published in final edited form as:
Microvasc Res. 2013 May ; 87: 75–82. doi:10.1016/j.mvr.2013.02.002.

Intussusceptive Remodeling of Vascular Branch Angles in Chemically-Induced Murine Colitis

Maximilian Ackermann[1], **Akira Tsuda**[2], **Timothy W. Secomb**[3], **Steven J. Mentzer**[4], and **Moritz A. Konerding**[1]

[1]Institute of Fuctional and Clinical Anatomy, University Medical Center of the Johannes Gutenberg University, Mainz, Germany

[2]Molecular and Integrative Physiological Sciences, Harvard School of Public Health, Boston, MA

[3]Department of Physiology, University of Arizona, Tucson, AZ

[4]Laboratory of Immunophysiology, Brigham & Women's Hospital, Harvard Medical School, Boston MA

Abstract

Intussusceptive angiogenesis is a developmental process linked to both blood vessel replication and remodeling in development. To investigate the prediction that the process of intussusceptive angiogenesis is associated with vessel angle remodeling in adult mice, we systematically evaluated corrosion casts of the mucosal plexus in mice with trinitrobenzesulphonic acid (TNBS)-induced and dextran sodium sulfate (DSS)-induced colitis. The mice demonstrated a significant decrease in vessel angles in both TNBS-induced and DSS-induced colitis within 4 weeks of the onset of colitis ($p<.001$). Corrosion casts 28–30 days after DSS treatment were studied for a variety of detailed morphometric changes. The vessel diameter and interbranch distance were significantly increased in the descending colon ($p<.05$). Also consistent with vessel growth, intervascular distance was decreased in the descending colon ($p<.05$). In contrast, no statistically significant morphometric changes were noted in the ascending colon. The morphometry of the corrosion casts also demonstrated 1) a similar orientation of the remodeled angles within the XY coordinate plane of the mucosal plexus, and 2) alternating periodicity of remodeled and unremodeled vessel angles. We conclude that inflammation-associated intussusceptive angiogenesis in adult mice is associated with vessel angle remodeling. Further, the morphometry of the vessel angles suggests the influence of blood flow on the location and orientation of remodeled vessels.

Keywords

morphometry; scanning electron microscopy; remodeling; mucosal plexus

Correspondence: Dr. Steven J. Mentzer, Room 259, Brigham &Women's Hospital, 75 Francis Street, Boston, MA 02115, smentzer@partners.org.
†These authors contributed equally to this work.

Introduction

Blood vessel bifurcations are an essential structural feature of all vascular networks. In tree-like branching patterns, blood flow travels through the parent vessel into two smaller diameter daughter vessels. The ubiquity of this fluid transport system in nature has led to considerable theoretical work attempting to produce a theory of universal bifurcation design (LaBarbera, 1990). Many of these theories are based on the premise that vessel geometry is organized on the principle of economy. Most notably, “Murray’s law” is the hypothesis that vascular architecture is driven by functional optimization; namely, vascular design reflects the minimal amount of energy necessary to maintain and circulate the blood (Murray, 1926). Although “Murray’s law” is remarkably accurate in predicting the branching diameters of large vessels, it is less accurate in the microcirculation. Particularly in non-tree branching patterns, such as plexuses and arcades, vessel bifurcations demonstrate wide geometric variation that cannot be explained by simple cost functions.

An intriguing non-tree branching vessel pattern is observed in the colonic mucosal plexus (Miele et al., 2009; Tsuda et al., 2009; Turhan et al., 2007). The mucosal plexus is a quasi-polygonal planar network that encircles the colonic crypts. In normal circumstances, the mucosal plexus supplies nutrients to the highly metabolic digestive epithelium. In inflammatory conditions such as acute and chronic colitis, the mucosal plexus undergoes active intussusceptive angiogenesis resulting in a dramatic increase in mucosal vascularity (Konerding et al., 2010).

Intussusceptive angiogenesis is a well-characterized morphogenetic process in cancer, inflammation and regeneration in which a single vessel is split into two lumens (Konerding et al., 2012; Konerding et al., 2010). A distinguishing anatomic feature of intussusceptive angiogenesis is the intussusceptive pillar. The intussusceptive pillar is a 1–5 μm (Burri et al., 2004) transluminal tissue bridge that spans the vessel lumen; its small size typically requires corrosion casting and scanning electron microscopy (SEM) for visualization (Lee et al., 2011; Lee et al., 2010). Physical expansion or growth of the pillar along the vessel axis divides the lumen resulting in vascular duplication. In addition to vessel division, the intussusceptive pillar can rapidly change the geometry of the affected vessel branch path (Djonov et al., 2002; Kurz et al., 2003). Whether the intussusceptive pillar contributes to vessel angle remodeling in murine colitis is uknown.

In this report, we investigated the hypothesis that intussusceptive angiogenesis, previously observed in murine colitis (Konerding et al., 2010), was also associated with branch angle remodeling. Our results suggest that pillar formation in chemically-induced colitis leads to both intussusceptive angiogenesis and branch angle remodeling.

Methods

Mice

Male Balb/c (N=183) or C57B/6 (N=244) mice (Jackson Laboratory, Bar Harbor, ME), 25–33 g, were used in all experiments. The care of the animals was consistent with guidelines of the American Association for Accreditation of Laboratory Animal Care (Bethesda, MD).

Trinitrobenzesulphonic acid (TNBS) colitis

Because of strain-specific sensitivity to TNBS (Elson et al., 1996), BALB/c mice were used for TNBS experiments. The mouse abdomen was sheared and cleansed with water; 24 hours later, 36 μl of a 2.5% trinitrochlorobenzene (TNCB) (ChemArt, Germany) solution was sprayed onto a 1.5 cm diameter circular PhastTransfer Filter Paper (Pharmacia, Upsala, Sweden) in a 4:1 acetone:olive oil mixture. The antigen soaked filter paper was applied to

sheared abdomen with Tegaderm (3M, St. Paul, MN) for 24 hours. On day 0, and at 7 day intervals, 36 μl of TNBS was administered intrarectally. The mice were assessed daily for clinical signs and total body weight.

Dextran sodium sulphate (DSS) colitis

In C57/B6 mice, the dextran sodium sulfate (DSS) (TdB Consultancy AB, Uppsala, Sweden) model of colitis was similar to that described previously (Okayasu et al., 1990). Briefly, DSS was freshly prepared and added daily to the mice drinking water at a final concentration of 5%. The mice were assessed daily for clinical signs and total body weight. The DSS treatment was continued for 5 days then changed to water for the remainder of the experimental period.

Clinical assessment of colitis

Clinical parameters including total body weight were assessed daily (Ravnic et al., 2007a). Activity level and fur ruffling were scored daily on a 0 (normal) to 2 (severe) scale. A change in body weight was also assigned a clinical colitis score: > 5% of the baseline weight = 1 point; >10% = 2 points.

Scanning electron microscopy

Corrosion casting and scanning electron microscopy (SEM) was performed in both TNBS (N=32) and DSS (N=64) mice. After systemic heparinization, PBS perfusion and intravascular fixation with 2.5% buffered glutaraldehyde, the systemic circulation was perfused with 10–20 ml of Mercox (SPI, West Chester, PA) diluted with 20% methyl methacrylate monomers (Aldrich Chemical, Milwaukee, WI) as described previously (Ravnic et al., 2006). After complete polymerization, the tissues were harvested and macerated in 5% potassium hydroxide followed by drying and mounting for scanning electron microscopy. The microvascular corrosion casts were imaged after coating with gold in an argon atmosphere with a Philips ESEM XL30 scanning electron microscope (Eindhoven, Netherlands). In some mice, stereo-pair images were obtained using a tilt angle of 6 degrees. The quality of the filling of the corrosion casts was also checked by comparisons with the vascular densities in semithin light microscopic sections stained with methylene blue. The corrosion casts chosen for morphometric analysis demonstrated filling of the whole capillary bed from artery to vein without evidence of extravasation or pressure distension.

Measurement of branch angles and pillars

Similar to previous studies emphasizing angle geometry (Thomas et al., 2005), the method of branch angle morphometry was designed to be sensitive to variation at the apex of the bifurcation. In layered images, maximally-sized spheres were inscribed in each vessel at the bifurcation (Figure 1). Sequential spheres within each vessel were inscribed so that the surface of the sphere intersected the centerpoint of the preceding sphere. The centerline track of the first two spheres was used to define the vessel coordinates. In cases with unusual tortuosity, in which the centerline track did not project over the vessel lumen, a third or fourth sphere centerpoint was used. The bifurcation angle was measured as the angle between centerline tracks using digital morphometry software. To minimize bias, the vessel angles were measured by observers blinded to the experimental conditions. The mean value of the observers was recorded. Representative stereopairs of vascular casts were analyzed for the assessment of bifurcations showing features of intussusceptive angiogenesis. Tiny holes and small capillary loops with a diameter between 1–5 μm at the bifurcation angles were identified as pillars on each image area and were assessed related to all bifurcations.

Morphometric measurements

The measurements of vessel diameters (Ravnic et al., 2007b) as well as interbranch (Ravnic et al., 2005) and intervascular (Malkusch et al., 1995) distances were performed as previously described.

Statistical analysis

The statistical analysis was based on measurements in at least three different mice. The unpaired Student's t test for samples of unequal variances was used to calculate statistical significance. The data was expressed as mean ± one standard deviation. The significance level for the sample distribution was defined as $P<.01$.

Results

Intussusceptive angiogenesis in colitis

Two models of chemically-induced colitis (TNBS and DSS) were studied for 30 days. The clinical signs of colitis—such as ruffled fur, decreased activity and weight loss—were commonly observed 4 to 7 days after the onset of inflammation (Figure 2A). Similarly, the highest mortality was observed within the first 5 days (Figure 2B). Coincident with resolution of the clinically apparent colitis, intussusceptive pillars were observed at bifurcations within the mucosal plexus (Figure 2C). Visible as "holes" within the corrosion casts (Figure 2Ca, b), pillars were the structural feature that signaled the onset of intussusceptive angiogenesis (Konerding et al., 2010). Intussusceptive pillars at vessel bifurcations were significantly more prevalent in DSS-colitis mice than in control mice (13% versus 5%; $p<.001$); nonetheless, the presence of pillars in control mice suggested that intussusceptive processes (angiogenesis and angle remodeling) participate in morphostasis; that is, routine mucosal maintenance and repair.

Vessel angle remodeling in colitis

To investigate the prediction that the process of intussusceptive angiogenesis is associated with vessel angle remodeling, we systematically evaluated corrosion casts of the mucosal plexus after chemically-induced colitis (Figure 3). The mice with chemically-induced colitis demonstrated a significant decrease in vessel angles in both TNBS-induced (Figure 3A,B) and DSS-induced (Figure 3C,D) colitis ($p<.001$). The distribution of the vessel angles differed slightly between DSS and TNBS colitis. Because of the effect of the vehicle alone on TNBS-induced vessel angles, subsequent experiments were restricted to the DSS treatment.

Morphometry of vessel angle remodeling

Corrosion casts 28–30 days after DSS treatment were studied for a variety of detailed morphometric changes. The vessel diameter, previously reported as a consequence of acute colitis (Ravnic et al., 2007b), was persistent in the descending colon (Figure 4); however, there was no difference in ascending colon vessel diameters. Interbranch distance, a morphometric measurement reflecting longitudinal growth, demonstrated a similar spatial dependence; that is, only the descending colon demonstrated an increase in interbranch distance (Figure 5). Finally, intervascular distance, a morphometric measure of vascular density, demonstrated an overall decrease in intervascular distance in the descending colon (Figure 6)—a finding compatible with previous observations of enhanced angiogenesis (Konerding et al., 2010).

Vessel angle orientation

The morphometry of the corrosion casts also suggested the influence of blood flow. In regions of the mucosal plexus supplied by bridging vessels (Turhan et al., 2007), the remodeled vessel angles demonstrated a similar orientation (Figure 7A). Assuming 3 possible orientations of the remodeled vessel angles in the X–Y coordinate plane, the unidirectional orientation of vessel angles was highly significant (Figure 7B and C; $p<.001$). Also, vessel angle remodeling was not observed at every bifurcation, but often appeared to occur at alternating bifurcations. This pattern is consistent with the periodic variations predicted by the influence of converging and diverging blood flow (Figure 7D)(Lee et al., 2010).

Discussion

In this study, we applied a method of vessel morphometry uniquely sensitive to branch angles, to the investigation of corrosion casts of the mucosal plexus 4 weeks after the onset of chemically-induced colitis. In a time course similar to intussusceptive angiogenesis, a subset of bifurcations demonstrated significant remodeling of the vessel branch angle. The remodeling was morphologically distinguishable from intussusceptive duplication. In addition, the spatial orientation and the periodicity of the remodeled angles suggested that remodeling was a response to regional flow patterns. We conclude that pillar formation in two models of chemically-induced colitis leads to both intussusceptive angiogenesis and branch angle remodeling.

A contribution of this study was the application of a morphometric method capable of defining branch angles at the bifurcation. Our previous attempts to characterize branch angles in the mucosal plexus emphasized the dominant linear segment of the mucosal capillary (Ravnic et al., 2005) and underestimated the acute angle remodeling defined here. We suspect that our current method of defining vessel angle remodeling can be applied to a variety of tissues; a similar method has already been applied to the carotid artery bifurcation (Thomas et al., 2005). An additional benefit of our current approach was the characterization of the orientation of the remodeled vessel angle. Because our morphometry software application uses a constant reference for the angle calculation, the exported data revealed a consistent trend; namely, the remodeled vessel angles within a region of mucosa, demonstrated a similar orientation relative to the X–Y coordinate plane of the plexus. The spatial orientation of remodeled vessel angles was consistent with the regional bridging vessel architecture (Turhan et al., 2007) and flow patterns (Tsuda et al., 2009) previously described. Together, the underlying mucosal plexus microarchitecture, the spatial distribution of angle remodeling, as well as the orientation and periodicity of the remodeled angles, suggests a mechanism of branch angle remodeling that was responsive to intraluminal blood flow.

A reproducible observation in these studies was the morphologic adaptations in the colon

There are two major limitations of this study. First, the time course of remodeling did not permit the direct examination of the remodeling process; that is, the experimental conclusions necessarily depended upon statistical and morphometric inference. Alternative explanations include a remodeling process that is initiated not at the intussusceptive pillar, but at the bifurcation apex. In this explanation, the remodeled vessel angle would be an extension of the vessel bifurcation rather than the physical expansion of the intussusceptive pillar. We suspect this alternative is unlikely because the corrosion casts of the remodeled bifurcations demonstrated extended luminal apposition (so-called “parallel segments”) characteristic of pillar remodeling (Baumbach and Ghoneim, 1993; Dosso et al., 1999; Komai et al., 2005) and uncharacteristic of systemic arterial remodeling (Djonov et al.,

2001; Djonov et al., 2000; Kurz et al., 2003). In addition, the branch angle remodeling occurred within an identical time frame and with comparable spatial distribution to intussusceptive angiogenesis—both processes induced by the same inflammatory stimulation.

Second, the accuracy of corrosion cast morphometry was limited by SEM projection distortion (Minnich and Lametschwandtner, 2000). Ideally, the planar mucosal plexus would be set normal to the scanning beam. With normal projection, the image magnification would be identical in any direction and the shape of the vessels in the corrosion cast would be accurately reproduced. A less accurate reproduction is obtained when the plane of the mucosal plexus is tilted. The projection of the scan line on the projection plane results in projection distortion or “image foreshortening.” Although projection distortion was present in the images used in our study, the deviations from a perpendicular SEM orientation—largely random and present in both colitis and control corrosion cast images—were unlikely to significantly influence the observed differences.

An interesting observation was the spatial dependence of the dominant vascular changes during prolonged colitis; that is, the changes in diameter, interbranch and intervascular distance were most notable in the descending colon. The selective changes in the descending colon were irrespective of hapten chemistry (TNBS versus DSS) or mode of administration (oral versus rectal instillation). The consistency of these findings suggests that the mucosal plexus vessels in the descending colon were qualitatively different from mucosal vessels in more proximal regions of the colon. Alternatively, the differential response in the descending colon may reflect a qualitatively distinctive immune response. In either case, the descending colon is the region most likely to yield insights into the process of inflammation-induced vascular adaptations in murine colitis.

Branch angle remodeling as a result of intussusceptive pillar extension has been postulated in computational (Filipovic et al., 2009), in vitro (Turhan et al., 2008) and in vivo (Makanya et al., 2009) models of intussusceptive angiogenesis. In the case of branch angles, pillar-mediated remodeling results in a narrowing of the branch angle. The subsequent alterations of flow streamlines may contribute to minimizing the amount of energy necessary to maintain and circulate the blood (Murray, 1926). Alternatively, the distinct flow streamlines as a result of a narrow branch angle may contribute to downstream pillar extension with the potential conseqeunce of vessel duplication (Konerding et al., 2010) or pruning (Lee et al., 2011). In any case, a major contribution of this study is the anatomic and morphometric evidence of branch angle remodeling in an adult animal.

In previous studies of intussusceptive pillars in the chicken CAM, we have noted that pillars form in areas of converging flow and appear to be shaped by blood flow (Lee et al., 2011; Lee et al., 2010). Our findings in the mouse colitis model are consistent with these observations. Pillars formed at the vessel junctions and were rarely observed in the intervening vessel segments. Although the flow direction is difficult to infer from the corrosion casts, the periodicity of the branch angle modification in the quasi-polygonal mucosal plexus reflected an alternating pattern of modified and unmodified branch angles. This pattern would be consistent with converging and diverging flow in the mucosal plexus. Further, our observation that pillar extension reflects the flow stream (Lee et al., 2011) is also supported by observations in the colon. In both branch angle remodeling and vessel duplication, the pillars appeared to extend along the vessel axis.

Finally, we have demonstrated both branch angle remodeling and intussusceptive angiogenesis within weeks after the onset of colitis. These findings provide support for the concept that dynamic structural changes in the microcirculation are a common feature in

colitis. We speculate that these changes have been underappreciated because of the limited spatial and temporal reference frames. Structural changes in the microcirculation are difficult to recognize in traditional 2-dimensional histologic sections. Similarly, the prolonged inflammation (3–4 weeks) is beyond the timeframe of most experimental approaches. Our observations suggest that structural adaptations occur in response to inflammation. It is also possible that inflammation may be prolonged or promoted by these structural changes. Further work will be necessary to illuminate the dynamic interaction between structural adaptations and inflammation.

Acknowledgments

Supported in part by NIH Grant HL47078 and HL75426

Abbreviations

2D	2-dimensional
3D	3-dimensional
CFSE	5-(and-6)-carboxyfluorescein diacetate, succinimidyl ester
DSS	dextran sodium sulphate
FITC	isothiocyanate
TNBS	2,4, 6-trinitrobenzenesulfonic acid
TNCB	2,4,6-trinitrochlorobenzene

References

Baumbach GL, Ghoneim S. Vascular remodeling in hypertension. Scanning Microsc. 1993; 7:137–42. [PubMed: 8316787]

Burri PH, et al. Intussusceptive angiogenesis: its emergence, its characteristics, and its significance. Dev Dyn. 2004; 231:474–88. [PubMed: 15376313]

Djonov V, et al. Vascular remodelling during the normal and malignant life cycle of the mammary gland. Microsc Res Tech. 2001; 52:182–9. [PubMed: 11169866]

Djonov V, et al. Intussusceptive angiogenesis: its role in embryonic vascular network formation. Circ Res. 2000; 86:286–92. [PubMed: 10679480]

Djonov VG, et al. Optimality in the developing vascular system: branching remodeling by means of intussusception as an efficient adaptation mechanism. Dev Dyn. 2002; 224:391–402. [PubMed: 12203731]

Dosso AA, et al. Remodeling of retinal capillaries in the diabetic hypertensive rat. Invest Ophthalmol Vis Sci. 1999; 40:2405–10. [PubMed: 10476809]

Elson CO, et al. Hapten-induced model of murine inflammatory bowel disease: mucosa immune responses and protection by tolerance. J Immunol. 1996; 157:2174–85. [PubMed: 8757344]

Filipovic N, et al. Computational flow dynamics in a geometric model of intussusceptive angiogenesis. Microvasc Res. 2009; 78:286–293. [PubMed: 19715707]

Komai Y, et al. Capillary angiogenesis and remodeling induced in rat limb by arteriovenous shunting. Clin Hemorheol Microcirc. 2005; 32:199–208. [PubMed: 15851839]

Konerding MA, et al. Spatial dependence of alveolar angiogenesis in post-pneumonectomy lung growth. Angiogenesis. 2012; 15:23–32. [PubMed: 21969134]

Konerding MA, et al. Inflammation-induced intussusceptive angiogenesis in murine colitis. Anat Rec. 2010; 293:849–857.

Kurz H, et al. Angiogenesis and vascular remodeling by intussusception: from form to function. News Physiol Sci. 2003; 18:65–70. [PubMed: 12644622]

LaBarbera M. Principles of design of fluid transport systems in zoology. Science. 1990; 249:992–1000. [PubMed: 2396104]

Lee GS, et al. Intravascular pillars and pruning in the extraembryonic vessels of chick embryos. Developmental Dynamics. 2011; 240:1335–1343. [PubMed: 21448976]

Lee GS, et al. Blood flow shapes intravascular pillar geometry in the chick chorioallantoic membrane. J Angiogenes Res. 2010; 2:11–20. [PubMed: 20609245]

Makanya AN, et al. Intussusceptive angiogenesis and its role in vascular morphogenesis, patterning, and remodeling. Angiogenesis. 2009; 12:113–23. [PubMed: 19194777]

Malkusch W, et al. A simple and accurate method for 3-D measurements in microcorrosion casts illustrated with tumour vascularization. Anal Cell Pathol. 1995; 9:69–81. [PubMed: 7577757]

Miele LF, et al. Blood flow patterns spatially associated with platelet aggregates in murine colitis. Anat Rec. 2009; 292:1143–1153.

Minnich B, Lametschwandtner A. Lengths measurements in microvascular corrosion castings: two-dimensional versus three-dimensional morphometry. Scanning. 2000; 22:173–7. [PubMed: 10888123]

Murray CD. The physiological principle of minimum work applied to the angle of branching of arteries. Journal of General Physiology. 1926; 9:835–841. [PubMed: 19872299]

Okayasu I, et al. A novel method in the induction of reliable experimental acute and chronic ulcerative colitis in mice. Gastroenterology. 1990; 98:694–702. [PubMed: 1688816]

Ravnic DJ, et al. Vessel painting of the microcirculation using fluorescent lipophilic tracers. Microvasc Res. 2005; 70:90–96. [PubMed: 16095629]

Ravnic DJ, et al. Murine microvideo endoscopy of the colonic microcirculation. J Surg Res. 2007a; 142:97–103. [PubMed: 17612562]

Ravnic DJ, et al. Inflammation-responsive focal constrictors in the mouse ear microcirculation. J Anat. 2006; 209:807–816. [PubMed: 17118067]

Ravnic DJ, et al. Structural adaptations in the murine colon microcirculation associated with hapten-induced inflammation. Gut. 2007b; 56:518–523. [PubMed: 17114297]

Thomas JB, et al. Variation in the carotid bifurcation geometry of young versus older adults: implications for geometric risk of atherosclerosis. Stroke. 2005; 36:2450–6. [PubMed: 16224089]

Tsuda A, et al. Bimodal oscillation frequencies of blood flow in the inflammatory colon microcirculation. Anat Rec. 2009; 292:65–72.

Turhan A, et al. Bridging mucosal vessels associated with rhythmically oscillating blood flow in murine colitis. Anat Rec. 2007; 291:74–92.

Turhan A, et al. Effect of intraluminal pillars on particle motion in bifurcated microchannels. In Vitro Cell Dev Biol. 2008; 44:426–433.

Highlights

- Intussusceptive pillars were demonstrated in an adult mouse colitis model.
- Corrosion casting demonstrated vessel angle remodeling in the colitis mice after 4 weeks.
- Descending colon vessels selectively demonstrated evidence of remodeling and growth.
- The orientation and periodicity of the remodeling suggested the influence of blood flow.

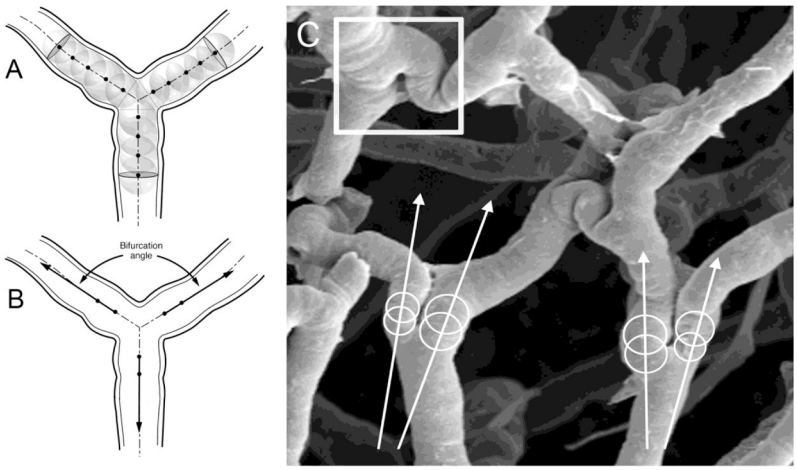

Figure 1.

The method of branch angle morphometry was designed to be sensitive to geometric variation at the apex of the bifurcation. A) Maximally-sized spheres were inscribed in each vessel at the bifurcation. Sequential spheres within each vessel were inscribed so that the surface of the sphere intersected the centerpoint of the preceding sphere. B) The centerline tract of the first two spheres was used to define the vessel coordinates. C) Example of two branch angles in colon mucosal plexus vessels. Note the intussusceptive pillar (square).

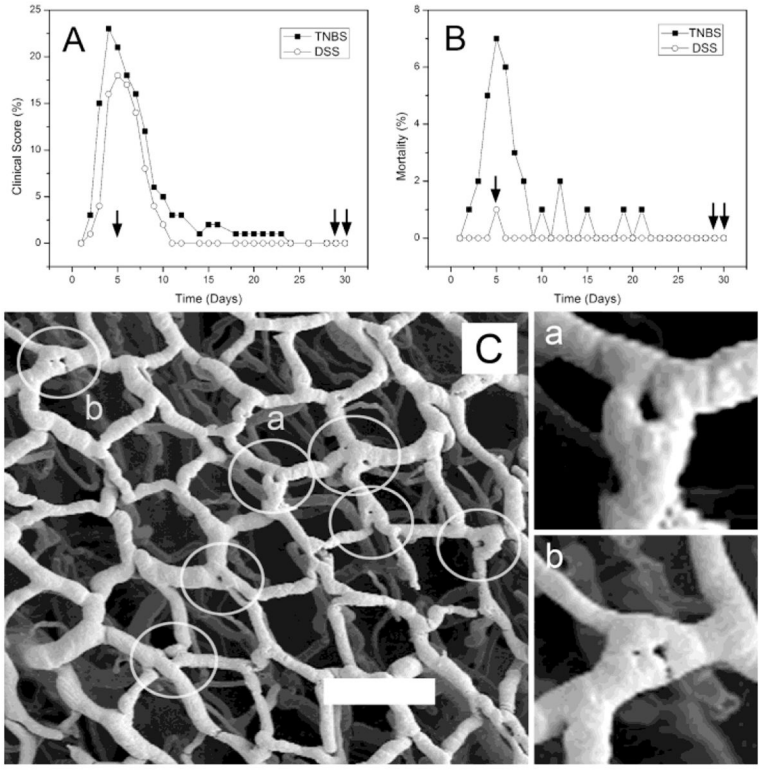

Figure 2.

The stimulation of intussusceptive angiogenesis by chemically-induced colitis. A) Frequency distribution of mice with a colitis score (see Methods) greater than 1 for TNBS- and DSS-induced colitis. Single arrow shows the timing of corrosion casts demonstrating intussusceptive pillars; double arrows identify the timing of corrosion casts examined for branch angle remodeling. B) Frequency distribution of deaths after the onset of TNBS- or DSS-induced colitis (TNBS N=100; DSS N=100). C) Corrosion casts of the mucosal plexus (descending colon) 5 days after the onset of TNBS-induced colitis. Circles identify “holes” that demonstrate the site of intussusceptive pillars. Two of the vessel bifurcations (a,b) are shown in higher magnification. Bar = 150 μm.

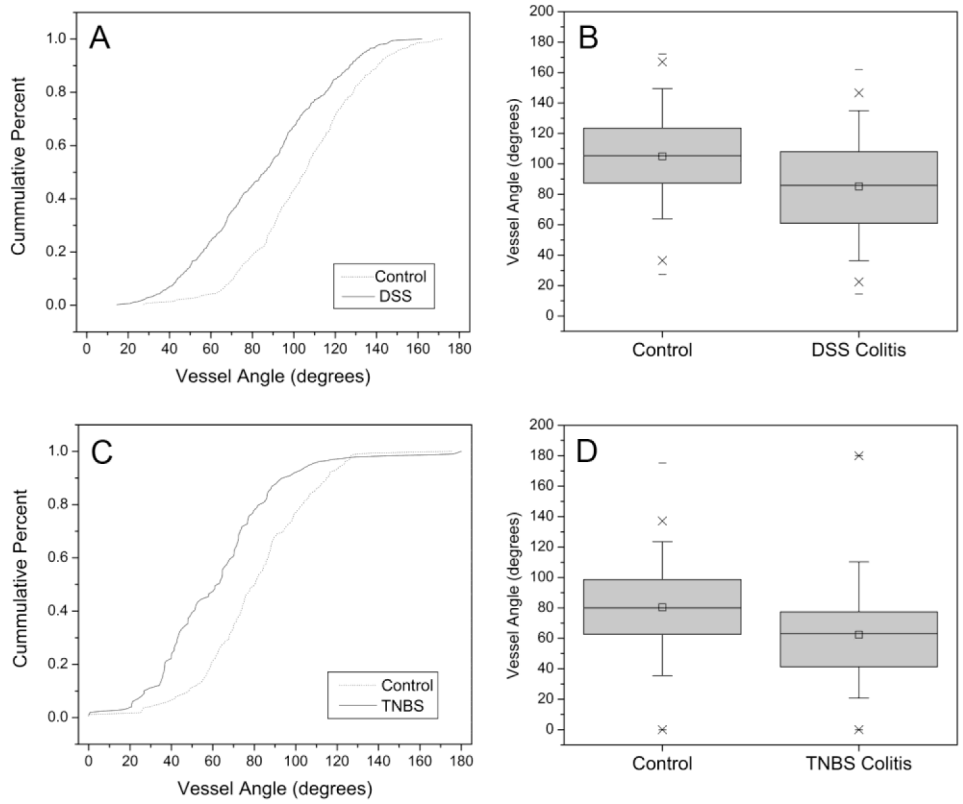

Figure 3.

The branch angles were measured in both DSS-induced (A,B) and TNBS- induced (C,D) colitis. The branch angles (N=750) of the DSS-induced colitis were examined by stereo-pair SEM morphometry; branch angles (N=350) of the TNBS-induced colitis mice were examined using 2D planar images. In the TNBS mice measurements, two investigators, blinded to the conditions, measured the bifurcation angle using the geometric technique (see Methods) to control for potential projection-dependent distortions. The median value between investigators was calculated and the histogram plotted for both colitis (square) and control (circle) mice ($p<.001$, t-test for samples of unequal variance).

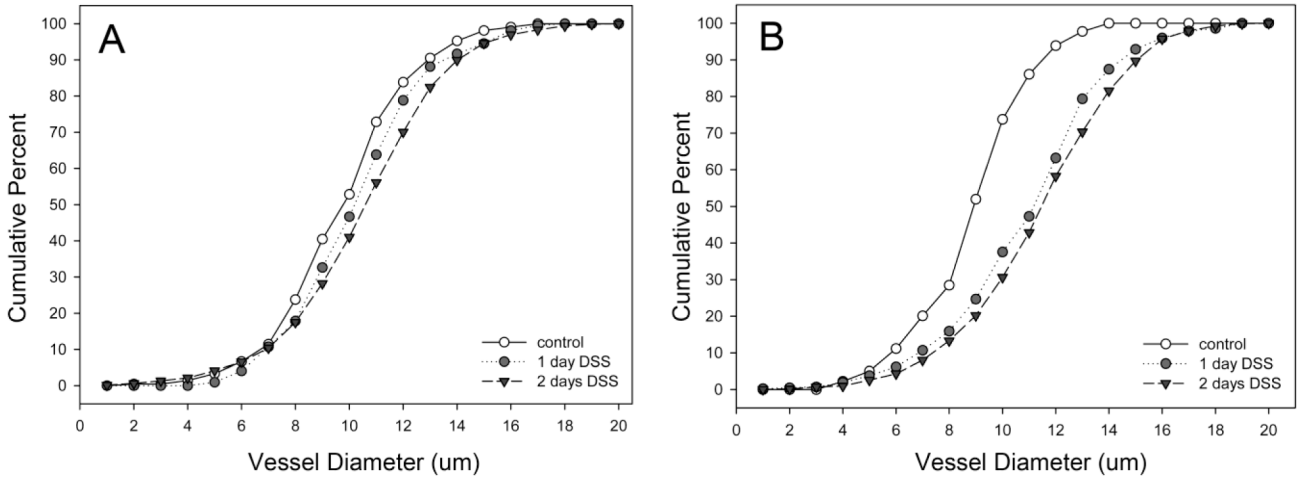

Figure 4.

The diameters of mucosal plexus vessels in the ascending (A) and descending (B) colons in DSS colitis. Murine colitis was stimulated with either 1 or 2 days of DSS exposure. At 28–30 days, corrosion casting demonstrated a significant increase in vessel diameter in the descending colon; there was no significant change in the ascending colon.

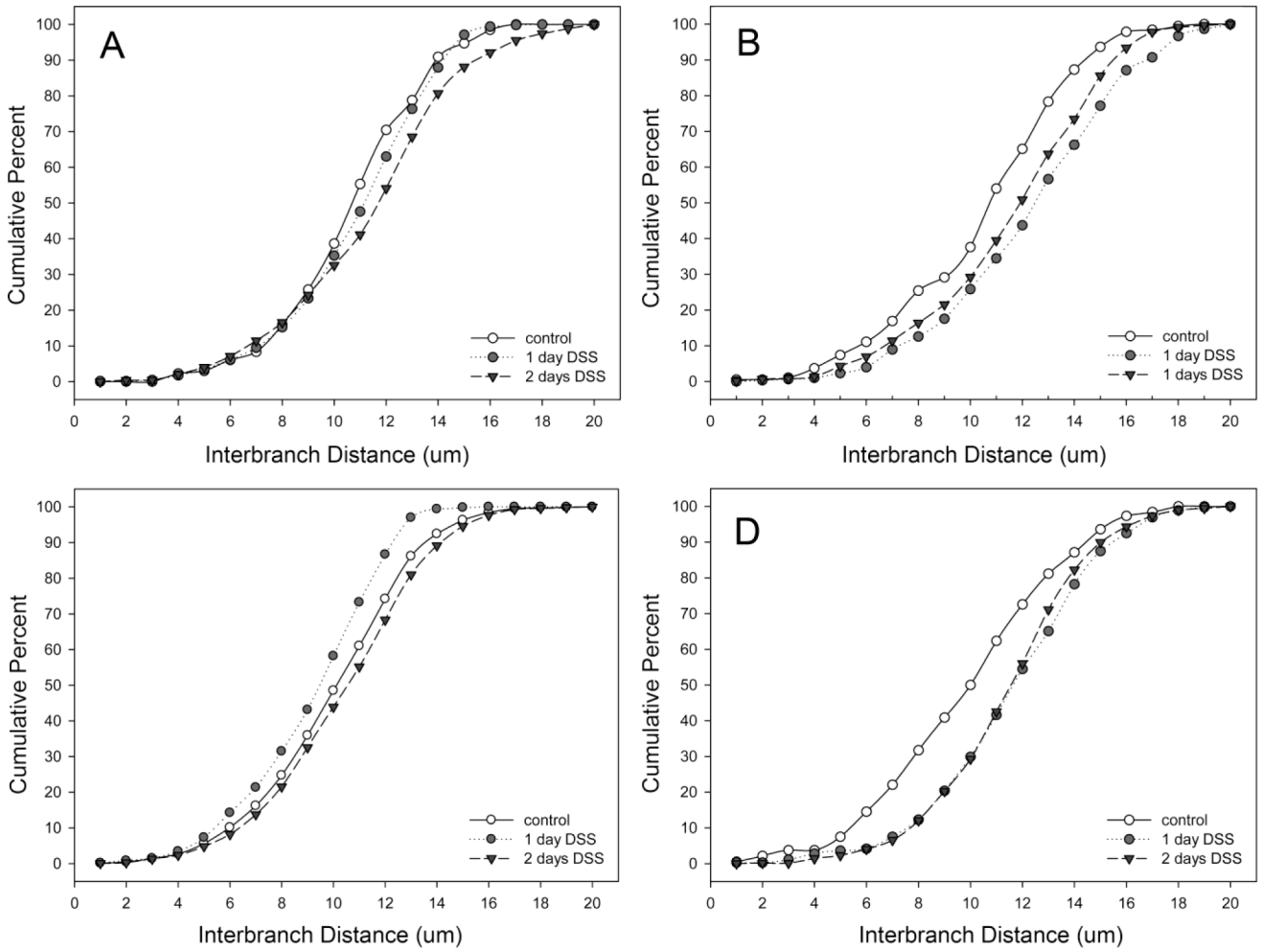

Figure 5.

The interbranch distance of mucosal plexus vessels in the cecum (A), ascending (B), transverse (C) and descending (D) colons in DSS colitis. Murine colitis was stimulated with either 1 or 2 days of DSS exposure. At 28–30 days, corrosion casting demonstrated a significant increase in interbranch distance in the descending colon; there was no significant change in the cecum, ascending or transverse colon. Of note, the control values in the transverse colon panel (C) represent aggregate control values from all regions.

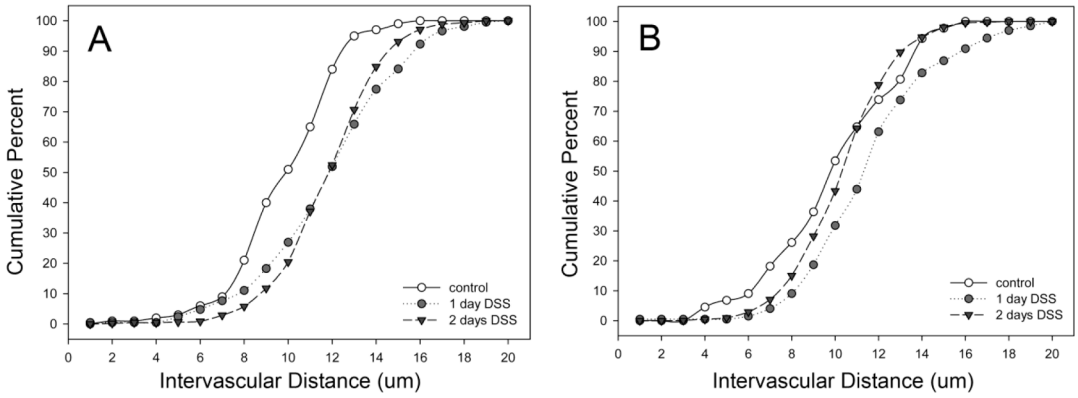

Figure 6.

The intervascular distance between mucosal plexus vessels in the ascending (A) and descending (B) colons in DSS colitis. Murine colitis was stimulated with either 1 or 2 days of DSS exposure. At 28–30 days, corrosion casting demonstrated a significant decrease in vessel distance in the descending colon; there was an increased distance in the ascending colon.

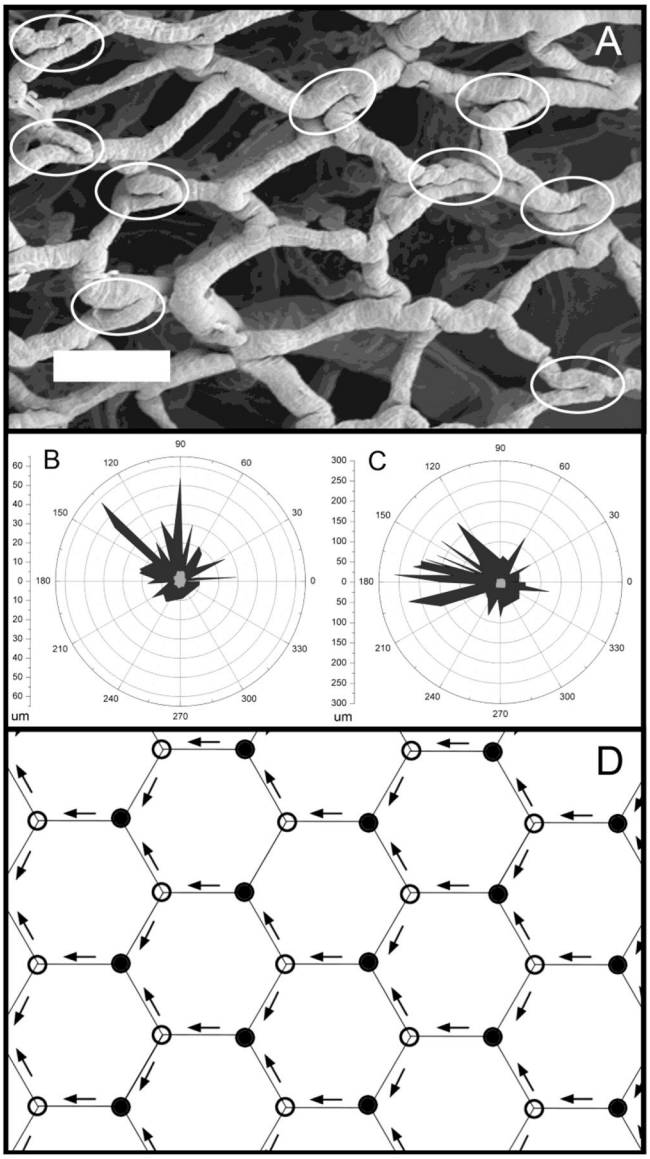

Figure 7.

The orientation of remodeled branch angles. A) A SEM photomicrograph of a corrosion cast obtained 30 days after the onset of TNBS-induced colitis (bar=100um). Acute branch angles, likely reflecting structural remodeling, are highlighted (elipses). Note the similar length and orientation of the parallel segments within the highlighted regions; specifically, the parallel segements of vessels at the vessel bifurcation. Two other examples (N=2 mice) of nonrandom remodeling are shown in the polar graphs (B,C). The length and orientation of the parallel segments are shown for colitis (black) and control (gray) mice. D) Schematic illustration of the periodic variation in converging (closed circles) and diverging (open circles) bifurcations created by a unidirectional flow field (arrows) in the colon mucosal plexus.